Unstable argininosuccinate lyase in variant forms of the urea cycle disorder argininosuccinic aciduria

ARTICLE *in* JOURNAL OF INHERITED METABOLIC DISEASE · MARCH 2015

Impact Factor: 3.37 · DOI: 10.1007/s10545-014-9807-3 · Source: PubMed

7 AUTHORS, INCLUDING:

Liyan Hu
University of Zurich
14 PUBLICATIONS **30** CITATIONS
SEE PROFILE

Amit V Pandey
Universität Bern
84 PUBLICATIONS **1,818** CITATIONS
SEE PROFILE

Sandra Eggimann
Universität Bern
8 PUBLICATIONS **21** CITATIONS
SEE PROFILE

Jean-Marc Nuoffer
Universität Bern
81 PUBLICATIONS **660** CITATIONS
SEE PROFILE

J Inherit Metab Dis
DOI 10.1007/s10545-014-9807-3

ORIGINAL ARTICLE

Unstable argininosuccinate lyase in variant forms of the urea cycle disorder argininosuccinic aciduria

Liyan Hu · Amit V. Pandey · Cécile Balmer · Sandra Eggimann · Véronique Rüfenacht · Jean-Marc Nuoffer · Johannes Häberle

Received: 8 July 2014 / Revised: 11 December 2014 / Accepted: 19 December 2014

Abstract Loss of function of the urea cycle enzyme argininosuccinate lyase (ASL) is caused by mutations in the *ASL* gene leading to ASL deficiency (ASLD). ASLD has a broad clinical spectrum ranging from life-threatening severe neonatal to asymptomatic forms. Different levels of residual ASL activity probably contribute to the phenotypic variability but reliable expression systems allowing clinically useful conclusions are not yet available. In order to define the molecular characteristics underlying the phenotypic variability, we investigated all *ASL* mutations that were hitherto identified in patients with late onset or mild clinical and biochemical courses by ASL expression in human embryonic kidney 293 T cells. We found residual activities >3 % of ASL wild type (WT) in nine of 11 ASL mutations. Six ASL mutations (p.Arg95Cys, p.Ile100Thr, p.Val178Met, p.Glu189Gly, p.Val335Leu, and p.Arg379Cys) with residual activities ≥16 % of ASL WT showed no significant or less than twofold reduced K_m values, but displayed thermal instability. Computational structural analysis supported the biochemical findings by revealing multiple effects including protein instability, disruption of ionic interactions and hydrogen bonds between residues in the monomeric form of the protein, and disruption of contacts between adjacent monomeric units in the ASL tetramer. These findings suggest that the clinical and biochemical course in variant forms of ASLD is associated with relevant residual levels of ASL activity as well as instability of mutant ASL proteins. Since about 30 % of known ASLD genotypes are affected by mutations studied here, ASLD should be considered as a candidate for chaperone treatment to improve mutant protein stability.

Communicated by: Carlo Dionisi-Vici

Jean-Marc Nuoffer and Johannes Häberle contributed equally to this study.

Electronic supplementary material The online version of this article (doi:10.1007/s10545-014-9807-3) contains supplementary material, which is available to authorized users.

L. Hu · C. Balmer · V. Rüfenacht · J. Häberle (✉)
Division of Metabolism, University Children's Hospital Zurich, Zurich 8032, Switzerland
e-mail: Johannes.Haeberle@kispi.uzh.ch

L. Hu · V. Rüfenacht · J. Häberle
Children's Research Center, Zurich 8032, Switzerland

A. V. Pandey
Pediatric Endocrinology, University Children's Hospital and Department of Clinical Research, University of Bern, Bern 3010, Switzerland

S. Eggimann · J.-M. Nuoffer
University Institute of Clinical Chemistry, University of Bern, Bern 3010, Switzerland

S. Eggimann · J.-M. Nuoffer
University Children's Hospital, University of Bern, Bern 3010, Switzerland

Published online: 17 March 2015

Introduction

Argininosuccinate lyase deficiency (ASLD, MIM #207900) is a rare autosomal-recessive urea cycle defect caused by mutations in the *ASL* gene encoding argininosuccinate lyase (ASL, EC 4.3.2.1, MIM *608310). ASL catalyzes the hydrolytic cleavage of argininosuccinate into arginine and fumarate and is, as part of the urea cycle, essential for ammonia detoxification and L-arginine synthesis (Brusilow and Horwich 2001). ASLD is considered the second most common urea cycle disorder (UCD) with an estimated incidence of 1:70,000 live births (Brusilow and Horwich 2001; Brusilow and Maestri 1996; Erez et al 2011a).

Biochemically, frequent findings in ASLD are hyperammonemia, an unfortunately unspecific sign, and

accumulation of argininosuccinic acid in tissues and body fluids (hence the synonymous term argininosuccinic aciduria, ASA), the latter being a specific and thus diagnostic biochemical marker (Solitare et al 1969; Tomlinson and Westall 1960, 1964). Levels of argininosuccinic acid in blood or urine vary between patients but there is no useful correlation between this marker and the severity of disease.

Clinically, patients with ASLD show a continuum from asymptomatic individuals over mild late onset forms to severe neonatal onset presentations with fatal hyperammonemic encephalopathy within the first few days of life (Erez et al 2011a). In contrast to most other UCDs, patients with ASLD seem to be affected by intellectual disability independent from the occurrence of hyperammonemic decompensations. In addition, for UCDs unusual and not fully understood complications of ASLD are the frequent findings of hepatic disease (Mori et al 2002; Zimmermann et al 1986) and of arterial hypertension (Brunetti-Pierri et al 2009) indicating to additional and possibly tissue-specific biological functions of ASL (Erez et al 2011b).

The *ASL* gene is located on chromosome 7cen-q11.2 and comprises 16 coding exons (NM_000048) (Linnebank et al 2002; O'Brien et al 1986; Todd et al 1989). The coding region of 1392 base pairs encodes a polypeptide of 464 amino acids (NP_000039), which forms as active enzyme a cytosolic homotetramer with a subunit molecular weight of ~52 kDa (O'Brien and Barr 1981; Palekar and Mantagos 1981). ASL is ubiquitously expressed in the human body with highest levels in the liver. A sequence on chromosome 22 was previously considered as a pseudogene (Linnebank et al 2002; O'Brien et al 1986) but later found to encode Ig-λ like mRNA (Linnebank et al 2002). Recently, an *ASL* pseudogene, which includes sequences from intron two to intron three, was identified upstream of the human *ASL* gene on chromosome 7 (Trevisson et al 2007). Mutations are spread almost all over the *ASL* gene and have recently been reviewed (Balmer et al 2014). Several attempts have been made to accomplish a prognostic marker and improve our understanding of the biochemical and clinical variability of ASLD. Enzymatic assays in erythrocytes (Mercimek-Mahmutoglu et al 2010; Tanaka et al 2002) or in cultured skin fibroblasts by direct (Tomlinson and Westall 1964) or indirect ASL measurement (Jacoby et al 1972; Kleijer et al 2002) have proven to be of some prognostic value for selected patients but lacked predictive reliability. Nevertheless, the indirect *ASL* assay by analysis of ^{14}C-citrulline incorporation in intact fibroblasts yielded sufficient sensitivity for detection of residual activities in variant forms of ASLD (Ficicioglu et al 2009; Kleijer et al 2002; Linnebank et al 2002) comprising patients with non-classical ASLD affected by only mild clinical symptoms, slight biochemical abnormalities, but no or only mild hyperammonemia.

In addition to measurements in patients' samples, there are some in vitro assays investigating naturally occurring *ASL* mutations in bacterial (*E. coli*) (Engel et al 2012; Sampaleanu et al 2001; Yu et al 2001), yeast (Barbosa et al 1991; Doimo et al 2012; Trevisson et al 2009) and eukaryotic (COS1-cells) (Walker et al 1990, 1997) expression systems. While identification of severely affected ASL proteins was feasible in all of these, there was overall no satisfying sensitivity for residual ASL activities and hence the predictive value was limited.

In the present study, we use our recently established eukaryotic expression system in human embryonic kidney 293 T cell lysates (Hu et al 2013) to investigate all naturally occurring *ASL* mutations up until now identified in patients with a variant biochemical or clinical phenotype in an attempt to better understand the cause of the broad variation in ASLD phenotypes. We found evidence for thermal instability as well as low expression levels pointing towards a hampered stability in these mutant ASL proteins, hereby contributing to our understanding of the underlying pathology in a part of ASLD.

Material and methods

Choice of *ASL* mutations

In this study, 13 known ASL sequence changes including the severe mutations p.Gln286Arg (c.857A>G) and p.Arg385Leu (c.1154G>T) as negative controls were investigated together with WT ASL (Fig. 1). Of the total 13 mutations, 11 (p.Arg12Gln (c.35G>A), p.Asp31Asn (c.91G>A), p.Arg95Cys (c.283C>T), p.Ile100Thr (c.299 T>C), p.Val178Met (c.532G>A), p.Glu189Gly (c.566A>G), p.Arg193Trp (c.577C>T), p.Val335Leu (c.1003G>T), p.Arg379Cys (c.1135C>T), p.Arg385Cys (c.1153C>T) and p.Arg445Pro (c.1334G>C)) are, according to literature (Balmer et al 2014), always associated with a variant clinical course, defined as late onset and/or mild clinical and biochemical phenotype. These 11 mutations as well as the two severe mutations compile to a list of over 60 genotypes that are provided, together with the available clinical information, in Supplemental Table 1. This list of 11 mutations comprises all known base pair substitutions meeting the criteria of a variant change (Table 1). The amino acid substitutions p.Ile100Thr and p.Arg379Cys belong to the two most frequent changes in ASLD that were initially described in Finish patients (Linnebank et al 2002). Notably, the mutations c.1153C>T (p.Arg385Cys) and c.1154G>T (p.Arg385Leu) affect the same amino acid but are reported to result in variant and severe clinical courses, respectively (Balmer et al 2014).

Construction of recombinant ASL mutations

Full-length *ASL* cDNA (1395 bp, RefSeq NM_000048.3) was cloned into the expression vector pcDNA3 (Invitrogen, Carlsbad, CA, USA) at *BamH*I and *Not*I restriction sites yielding

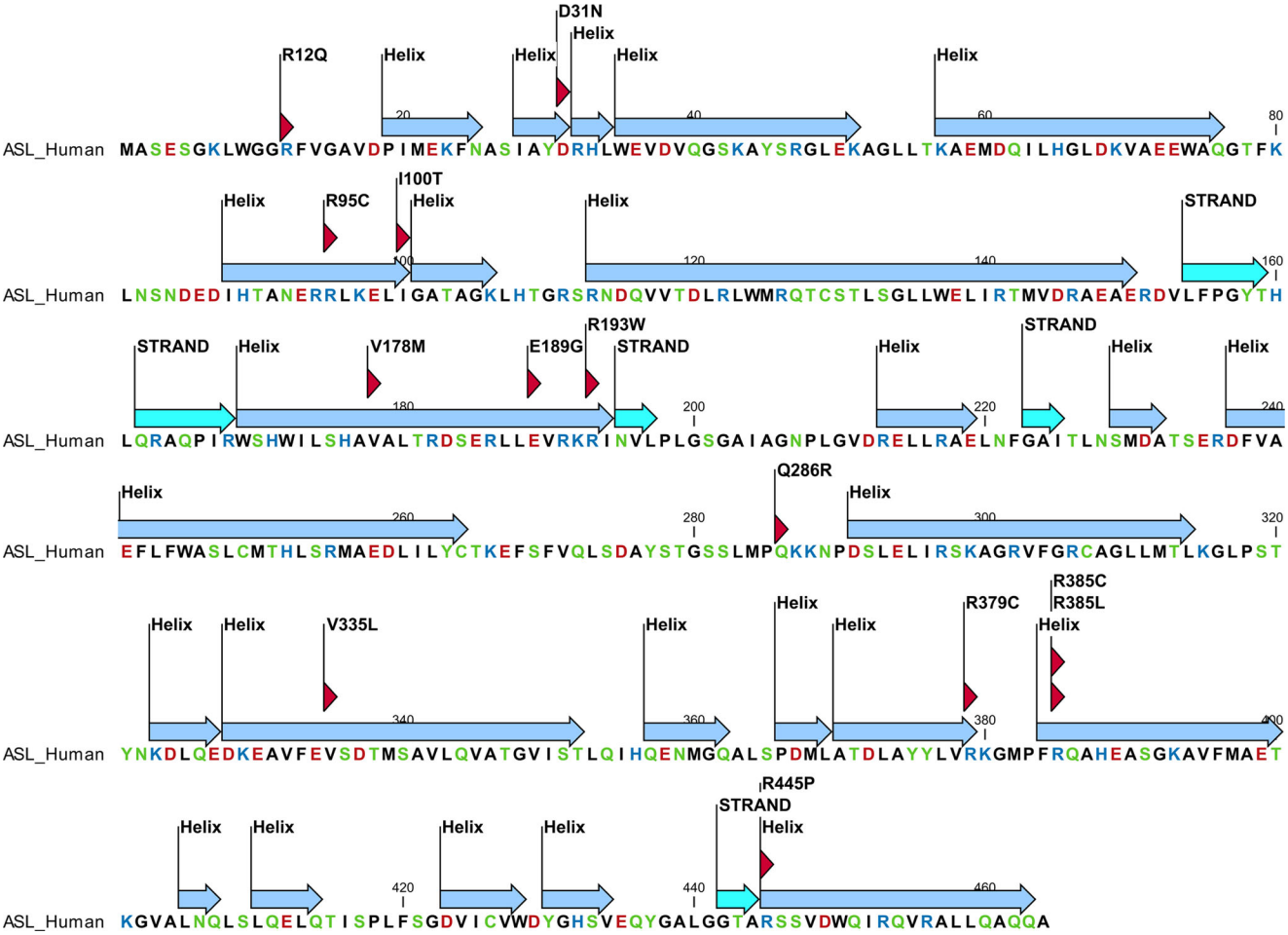

Fig. 1 Mutations in the ASL protein mapped onto the secondary structure of the human ASL protein sequence. Mutations are indicated with red triangles. Helices are shown in light blue and beta strands are shown as *cyan arrows*. Amino acids are coloured according to chemical properties, with aspartic and glutamic acids are in *red*, arginines and lysines in *blue* and aromatic amino acids are shown in *green*. Secondary structure information was extracted from the known crystal structures of ASL (PDB 1 K62) and figure was created with the program CLC Workbench. Sequence conservation information (presented in more detail in Supplementary Fig. 1) is indicated below the amino acids used in this study, H indicated high conservation and P indicates partial conservation

pcDNA3-ASL-WT (P-WT) as described previously (Hu et al 2013). The mutant plasmids were constructed based on P-WT by site-directed mutagenesis (Phusion Site-directed mutagenesis Kit, Finnzymes, Espoo, Finland) according to manufacturer's protocol. Oligonucleotide primers designed to achieve the respective point mutations are listed in Supplemental Table 2. PCR-products obtained after mutagenesis were subjected to *BamH*I (New England Biolabs, Beverly, MA, USA) digestion and their size compared to P-WT by gel electrophoresis. The PCR products with correct size were then transformed into chemically competent DH5$\alpha^{™}$-T1® *E.coli* cells (Invitrogen, Carlsbad, CA, USA) by using the heat shock method and selected by growth on ampicillin-containing (100 μg/ml) LB-agar. Screening-PCR with primers T7 forward [5′TAATACGACTCACTATAGGG3′] and Sp6 reverse [5′ATTTAGGTGACACTATAG3′] was used to identify positive clones. Then, mutant plasmids were isolated from *E. coli* and purified by using standard procedures (QIAprep spin column Miniprep Kit, Qiagen, Hombrechtikon, Switzerland). The yielded mutant plasmids (P-mutant) were named as P-R12Q, P-D31N, P-R95C, P-I100T, P-V178M, P-E189G, P-R193W, P-Q286R, P-V335L, P-R379C, P-R385C, P-R385L and P-R445P. All established constructs were confirmed by sequencing using the BigDye Terminator cycle sequencing kit V.1.1 (Applied Biosystems, ABI sequence).

Expression of ASL constructs in human embryonic kidney 293T cells

We have previously shown that 293 T cells were an ideal ASL expression system lacking endogenous ASL but allowing for high ectopic ASL expression (Hu et al 2013). Cells were grown, maintained and transiently transfected as described before (Hu et al 2013). In brief, 293 T cells were grown in Dulbecco's modified Eagle's medium+GlutaMAX (DMEM, Gibco, Paisley, UK) supplemented with 10 % fetal bovine

Table 1 Details of naturally occurring ASL missense mutations[a], clinical course and enzymatic characteristics of expressed recombinant mutant proteins

Mutation		Clinical course	ASL activity in the extract (± S.D.)[b]	ASL protein content[c]	Specific activity of pure ASL (± S.D.)[d]	V_{max} of pure ASL (± S.D.)[e]	K_m (± S.D.)[e]	V_{max}/K_m ratio[e]	T_m (± S.D.)[e]
Nucleotide level	Protein level		(mIU/mg)	(% of WT)	(% of WT)	(mIU/mg)	(mM)	(% of WT)	(°C)
WT	WT	–	1077.2±506.1	100	100±5.4	769.0±14.2	0.44±0.03	100	52.7±0.2
EV	EV	–	4.3±1.8	–	0.5±0.2	–	–	–	–
c.35G>A	p.R12Q	variant	41.7±4.8	125	4.3±0.5	n.d.	n.d.	n.d.	n.d.
c.91G>A	p.D31N	variant	20.1±2.2	88	2.0±0.7	n.d.	n.d.	n.d.	n.d.
c.283C>T	p.R95C	variant	70.6±31.7	37	18.0±5.7	99.2[f]±2.7	0.18f±0.02	32	46.5[f]±0.1
c.299 T>C	p.I100T	variant	880.8±361.1	91	86.6±24.6	488.0[f] ±15.1	0.46±0.06	61	48.5[f]±0.1
c.532G>A	p.V178M	variant	644.1±246.3	73	88.9±19.2	714.0[f]±14.1	0.44±0.04	93	49.9[f]±0.2
c.566A>G	p.E189G	variant	1012.9±411.7	97	91.4±15.3	669.3[f]±16.1	0.49±0.05	78	48.1[f]±0.1
c.577C>T	p.R193W	variant	18.9±9.9	37	4.1±1.3	n.d.	n.d.	n.d.	n.d.
c.857A>G	p.Q286R	severe	9.7±6.4	107	1.2±0.8	n.d.	n.d.	n.d.	n.d.
c.1003G>T	p.V335L	variant	553.8±135.3	104	46.4±21.0	443.6[f]±10.8	0.53±0.05	48	42.4[f]±0.5
c.1135C>T	p.R379C	variant	637.4±240.1	98	68.5±16.2	487.3[f]±9.0	0.25[f]±0.02	112	48.0[f]±0.1
c.1153C>T	p.R385C	variant	12.8±2.0	110	1.5±0.2	n.d.	n.d.	n.d.	n.d.
c.1154G>T	p.R385L	severe	10.3±3.3	99	1.3±0.4	n.d.	n.d.	n.d.	n.d.
c.1334G>C	p.R445P	variant	11.4±0.8	40	3.2±0.2	n.d.	n.d.	n.d.	n.d.

EV, empty vector; WT, wild-type

[a] All known genotypes to each missense mutation are published in (Balmer et al 2014) and are listed as well in Supplementary Table 1

[b] ASL activities were measured under standard conditions using 13.6 mM argininosuccinate and given as experimental activity versus the total protein content in the extract in mIU/mg protein

[c] ASL protein content was given as percentage of WT to estimate the expressed ASL mutant protein present in the extract compared to that of WT based on GAPDH by densitometry. It was determined by the following quotient: (ASL band for the mutant/GAPDH band for mutant)/(ASL band for WT/GAPDH band for WT) using Western blot analysis

[d] The specific activity of pure ASL given as percentage of WT was determined by the ratio of ASL mutant activity/ASL WT activity/ASL protein content indicating the relative enzyme activity of the expressed ASL mutant protein compared to that of the WT enzyme after normalization of the expressed ASL protein levels based on GAPDH by densitometry estimation. This was determined in each transfection under the same conditions in triple measurements from at least three independent transfection experiments, respectively

[e] V_{max} of pure ASL and K_m values were calculated by Michaelis-Menten equation and the melting temperature T_m (resulted as V_{50} value on Prism) by Boltzmann sigmoidal equation using GraphPad Prism 4 for curve fitting in triple measurements from the same experiment. V_{max} values of pure ASL were determined after normalization of the expressed ASL protein levels based on GAPDH by densitometry estimation using the same samples for kinetics assay

[f] Significant difference compared with ASL WT ($p<0.05$)±S.D.: standard deviation; n.d.: not determined

serum (FBS) and 1 % antibiotic/antimycotic solution (both PAA, Pasching, Austria) and maintained in an incubator containing 5 % CO_2 at 37 °C in a humidified atmosphere. A total of 7 μg of plasmid carrying ASL WT or the intended mutations was introduced into the cells in a 60 mm-dish format, using Lipofectamine™ LTX and PLUS™ Reagents (Invitrogen, Basel, Switzerland) according to manufacturer's instructions. The empty vector (EV) pcDNA3 was used as negative control.

Protein extraction and Western blot analysis

Cells were harvested 48 hours post-transfection and lysed in Lubrol WX lysis buffer containing 0.15 % (w/v) of Lubrol WX (Sigma Chemical Co., Poole, Dorset, UK) and 10 mM of Tris–HCl (pH 8.6) for 1 hour on ice. Cell lysates were then centrifuged at 16,873×*g* (14,000 rpm) at 4 °C for 15 min using Eppendorf microcentrifuge 5418. Protein concentrations in the supernatants (cell extracts) were determined by Bradford assay (Bradford 1976) using bovine serum albumin as standard.

Western blotting was performed as previously described (Laemmli 1970). Cell extracts (30 μg total protein) were separated by 10 % denaturing sodium dodecyl sulfate-polyacrylamide gel electrophoresis (SDS-PAGE) and subsequently transferred to nitrocellulose transfer membranes (Whatman GmbH, Dassel, Germany). The primary polyclonal antibody anti-ASL (GeneTex, Irvine CA, USA), recognizing

ASL residues 13 to 261 according to the manufacturer, was used at a dilution of 1:1000 and the horseradish peroxidase (HRP)-conjugated secondary antibody anti-rabbit (Santa Cruz Biotechnology, Santa Cruz CA, USA) was used at a dilution of 1:5000. Antibodies against glyceraldehyde-3-phosphate dehydrogenase (GAPDH) (Santa Cruz Biotechnology) served as loading control. ECL reagents (GE Healthcare, Glattbrugg, Switzerland) were used for chemiluminescent labelling to detect protein. To estimate expression levels of recombinant ASL mutations, densitometry analysis of bands detected by Western blotting was performed by using Carestream Molecular Imaging software (Carestream Health, Germany).

ASL enzymatic activity assay, kinetic study and thermal stability assay

The ASL enzymatic activity was determined spectrophotometrically in cell extracts after three independent transient transfections of P-WT or P-mutants, using a coupled assay with arginase and measuring urea production as described before (Engel et al 2012). In short, 100 μl of 34 mM argininosuccinate (argininosuccinic acid disodium salt hydrate) in water and 100 μl arginase (50 units) (both Sigma-Aldrich, Buchs, Switzerland) in 66.7 mM phosphate buffer (11.1 mM potassium dihydrogenphosphate and 55.6 mM disodium hydrogenphosphate, pH 7.5) were incubated at 37 °C for 5 min. Then 40 μl of cell extract (6 μg of total protein diluted in albumin buffer yielding 0.15 mg/ml of concentration for WT and all mutations except for p.Arg95Cys, in which we adapted protein quantity to 0.65 mg/ml according to low expression levels) and 10 μl phosphate buffer were incubated with the above reagents at 37 °C for 30 min. The reaction was stopped by adding perchloric acid at a final concentration of 2 %. In this assay, the measured extinctions are corrected with the extinctions of a blank containing all the reagents and cells as well as perchloric acid before the reaction started. The ASL enzyme activities are given as mIU/mg total protein indicating nmol of urea production/min/mg total protein and normalized according to the expressed ASL protein levels by densitometry analysis using GAPDH as control. The residual activities of ASL mutations are determined as percentage of ASL WT under the same conditions in triple measurements, respectively.

Kinetic studies and thermal stability assays were performed for ASL WT and mutations (p.Arg95Cys, p.Ile100Thr, p.Val178Met, p.Glu189Gly, p.Val335Leu and p.Arg379Cys) with residual ASL activities ≥18 % of ASL WT. The measured enzymatic activities were normalized according to the expressed ASL protein levels by densitometry using GAPDH as control. The kinetic parameters were determined by Michaelis-Menten analysis at ten different argininosuccinate concentrations after curve fitting using GraphPad Prism 4 (GraphPad Software, San Diego, CA, USA). For ASL thermal stability assay all ASL proteins were diluted at 0.15 mg/ml in albumin buffer (pH 7.4) and heated at different temperatures for 30 min in a PCR machine, and then immediately cooled down to 0 °C on ice followed by measuring ASL enzymatic activity as above (incubation temperatures in °C for WT: 37, 42, 47, 52, 54, 56, 57; p.Arg95Cys: 37, 40, 43, 45, 47, 49, 51; p.Ile100Thr, p.Glu189Gly and p.Val178Met: 37, 42, 47, 48.5, 50, 51.5, 53; p.Val335Leu: 37, 40, 42, 44, 46, 47, 48, 50; mutant p.Arg379Cys: 37, 42, 47, 48, 48.5, 50, 51, 51.5, 53). The mutant protein p.Arg95Cys, which is expressed less efficient and exhibited only low enzyme activity, was diluted at 0.65 mg/ml. The melting temperature T_m (resulted as V_{50} value on Prism) indicating the temperature at which 50 % of protein is inactivated, was determined by Boltzmann sigmoidal curve fitting of the data using GraphPad Prism 4 (GraphPad Software). All assays were carried out in triplicate using cell lysates from the same transfection experiment.

Structure models of ASL mutations

3D protein model and in-silico mutagenesis of ASL

The tetrameric 3D structure of ASL (NCBI NP_000039.2, Uniprot P04424) sequence (AA 1–464) was built using the in-silico mutagenesis of ASL structure (PDB 1 K62) as described previously (Hu et al 2013). Structural mutagenesis was performed with programs YASARA (Krieger et al 2004) and WHATIF (Vriend 1990). Side chains were optimized by molecular dynamic (MD) simulations. The geometry information for the tetramer assembly was extracted from the original crystallographic data. The final structure was refined by a 1000 ps (MD) simulation using AMBER 2003 force field and checked with the programs WHAT_CHECK (Hooft et al 1996), WHATIF (Vriend 1990), Verify3D (Bowie et al 1991; Luthy et al 1992), and Ramachandran plot analysis (Hooft et al 1997; Ramachandran et al 1963). Information about the residues located at the argininosuccinic acid binding pocket was extracted from the duck crystallin structure (PDB 1DCN) (Vallee et al 1999) using the program SiteEngines (Shulman-Peleg et al 2004, 2005). Structures were depicted with Pymol (www.pymol.org) and rendered as ray-traced images using the program POV-RAY (www.povray.org). Structural properties of the proteins were calculated by YASARA and WHATIF and general protein parameters were calculated with Expasy protein tools (www.expasy.ch).

Molecular dynamics simulation for model refinement

The MD simulations were performed using AMBER03 force field as described previously (Krieger et al 2004; Liu et al 2001). The simulation cell was filled with water, pH was fixed

to 7.4 and the electrostatic potentials were evaluated for water molecules in the simulation cell and adjusted by addition of sodium and chloride ions. The final MD simulations were then run with AMBER03 force field at 298 K, 0.9 % NaCl and pH 7.4 for 1000 ps to refine the models. The best models were selected for analysis and evaluation of the effect of mutations on monomer and tetramer structures. For the tetramer, mutations were created on either one or all four subunits to analyze different combinations of mutated and WT ASL monomers.

Predicting the effect of mutations on protein stability using site directed mutator (SDM)

The SDM tool (Topham et al 1997; Worth et al 2007) was used for predicting the effect of mutations on ASL protein stability. SDM software uses environment-specific substitution frequencies within homologous protein families to calculate a stability score. The mutant structures used for analysis were generated using the program ANDANTE (Smith et al 2007). SDM provides a pseudo delta G score for prediction of protein stability.

RNA structure and stability prediction

RNA structure and stability prediction was performed using the program RNAsnp (Sabarinathan et al 2013). A cutoff p value of 0.2 was used for predicting the effect on RNA stability. Both the global as well as local effects were evaluated for predicting the changes in the RNA structure upon mutations. The minimum free energy structures of the WT and mutant RNA were used to display the secondary structures in the graphic format.

Statistics

Statistical analyses were done using student one-tailed *T*-test using the program GraphPad Prism 4 (GraphPad Software) to describe the differences of K_m and V_{50} values in kinetic and thermal stability assays, respectively, between WT and mutant ASL with significant residual activities. Differences were considered as significant if the p value was <0.05.

Results

Expression of recombinant ASL WT and mutations in 293T cells

In order to investigate the molecular characteristics of all known naturally occurring ASL missense mutations associated with a variant clinical course in ASA patients (Balmer et al 2014), we first constructed the recombinant ASL WT and mutant plasmids followed by introducing them into 293 T cells, respectively. To check whether the recombinant diverse ASL mutations can be expressed at the protein level, Western blot analysis was performed under denaturing conditions which yielded expression of all recombinant ASL mutant proteins (Fig. 2a). More specific, a similar level of ASL expression as in WT was observed in all mutations except for p.Arg95Cys, p.Arg193Trp and p.Arg445Pro with lower protein yields (37, 37 and 40 % of WT after normalisation with loading control GAPDH by densitometry) (Table 1) indicating that these mutations are less stable at either protein or RNA level. We performed RNA secondary structure prediction to check whether substantial variations from the WT RNA were the cause of lower expression levels. Our analysis showed significant differences for the p.Arg193Trp (p-0.157) and p.Arg445Pro (p-0.118) variants (Fig. 3). Thus, combination of RNA and protein stability effects may be responsible for lower expression of some mutant proteins.

Residual ASL enzymatic activities in transfected 293T cell extracts

To determine whether the expressed ASL mutations have any residual enzyme activity, we performed ASL enzyme activity assays with the cell extracts used for Western blot analysis (summary of data in Table 1 and Fig. 2b). The residual enzymatic activities were normalized according to the expressed ASL protein levels by densitometry using GAPDH as control. There was no relevant endogenous ASL activity in cells transfected with EV. No significant residual activity (≤2 % of ASL WT) was observed in cells respectively transfected with two severe mutations p.Gln286Arg and p.Arg385Leu as well as with two variant mutations p.Asp31Asn and p.Arg385Cys, whereas cells expressing ASL WT yielded high enzymatic activity (Fig. 2b). Cells expressing the other nine variant mutations (p.Arg12Gln, p.Arg95Cys, p.Ile100Thr, p.Val178Met, p.Glu189Gly, p.Arg193Trp, p.Val335Leu, p.Arg379Cys and p.Arg445Pro) showed a residual activity >3 % of ASL WT. Surprisingly, six of them (p.Arg95Cys, p.Ile100Thr, p.Val178Met, p.Glu189Gly, p.Val335Leu and p.Arg379Cys) displayed a high level of ASL residual activity ≥16 % of ASL WT (Table 1 and Fig. 2b).

Kinetic study of variant mutations with high residual ASL activities

Next, we wanted to study the molecular pathology in ASA patients identified with variant mutations (p.Arg95Cys, p.Ile100Thr, p.Val178Met, p.Glu189Gly, p.Val335Leu and p.Arg379Cys) harbouring residual activities ≥16 % of ASL WT. Therefore, we analysed whether the kinetic parameters were impaired in these mutations using different concentrations of the substrate argininosuccinate (summary of data in

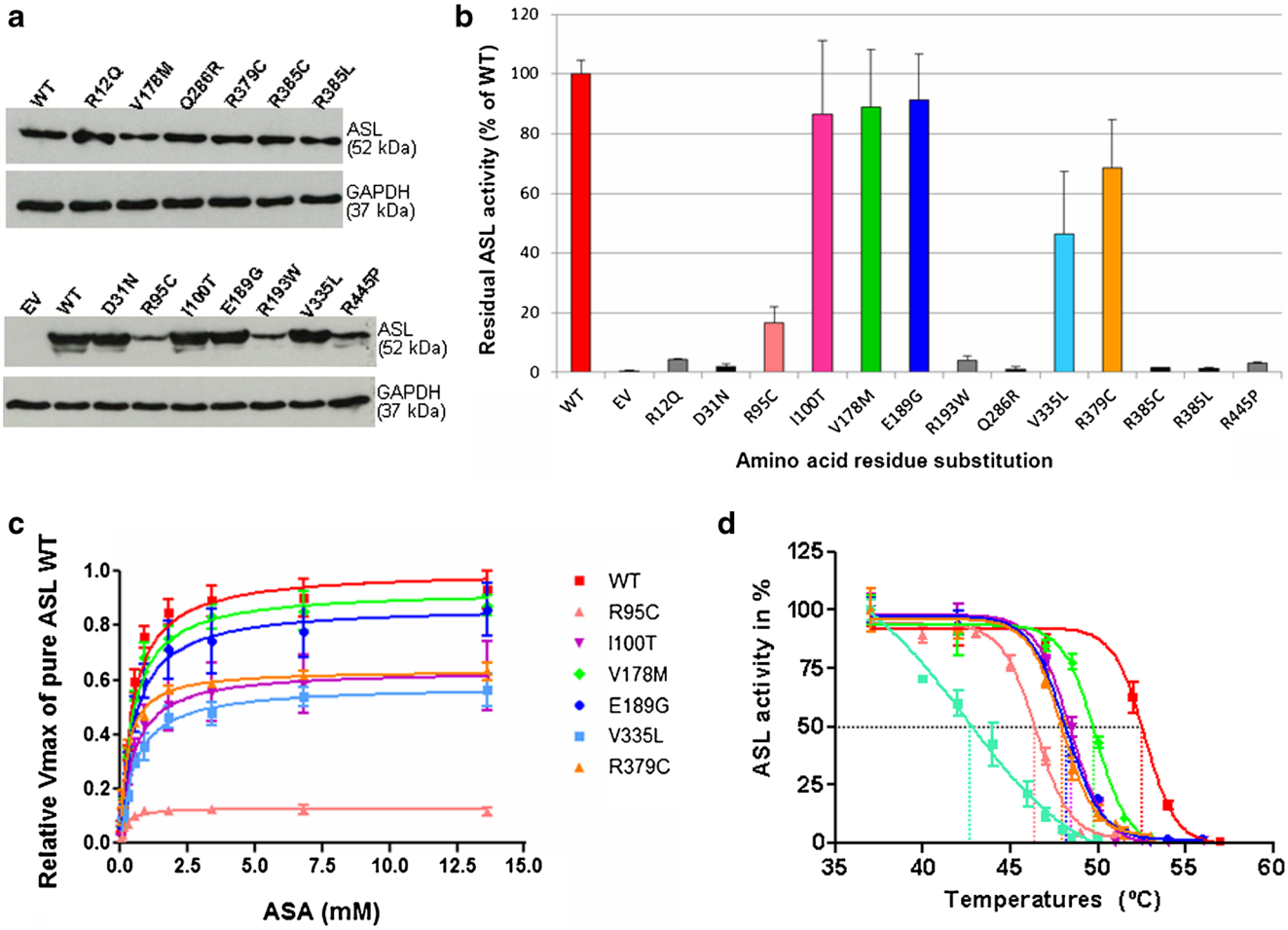

Fig. 2 Expression and enzymatic properties of the ASL WT and mutations. **a**: Expression of recombinant WT and mutant ASL in 293 T cells. These 293 T cells were transiently transfected with empty vector pcDNA3 (EV), recombinant ASL WT and mutant plasmids, respectively. ASL expression was detected by Western blot analysis using 30 μg of total protein separated by 10 % SDS-PAGE. GAPDH (37 kDa) served as loading control. **b**: Residual ASL activities of recombinant ASL proteins in 293 T cells. ASL enzymatic activity was measured under standard conditions using 13.6 mM argininosuccinate in cells transiently transfected EV or diverse ASL constructs (6 μg of whole cell extracts), respectively. The residual ASL activities are represented as a percentage of ASL WT activity yielded under the same conditions and normalized with GAPDH according to the expressed ASL protein levels by densitometry. ASL severe mutations (Q286R and R385L) and EV served as negative control and were marked in *black*. Nine variant changes yielded residual activities >3 % of ASL WT (in *red*) were marked in different colours: R95C in *salmon*, I100T in *purple*, V178M in *green*, E189G in *blue*, V335L in *cyan*, R379C in *orange*, and R12Q, R193W and R445P in *grey*. Two variant changes (D31N and R385C) yielded no significant residual activities (≤2 % of WT) and were also marked in *black*. All assays were carried out in triplicate measurements of at least three independent experiments, respectively. **c**: Kinetic study of recombinant ASL proteins showing significant residual activities. Kinetic study was performed for ASL WT and six variant changes (R95C, I100T, V178M, E189G, V335L, and R379C) (6 μg of whole cell extracts) with ≥18 % of WT activity using ten indicated different argininosuccinate concentrations (ranging from 0.045 to 13.6 mM), respectively. The measured enzymatic activities were normalized according to the expressed ASL protein levels by densitometry using GAPDH as control and represented as mIU/mg of whole cell extract. The kinetic parameters V_{max} given as relative value of 1 for ASL WT (referred to here as pure enzyme according to the normalized expressed ASL enzyme) and K_m in mM of argininosuccinate were determined by Michaelis-Menten analysis after curve fitting using GraphPad Prism 4. **d**: Thermal stability of recombinant ASL proteins with high residual activities. A total of 6 μg of protein diluted at 0.15 mg/ml (except for 26 μg of mutant R95C protein, which is expressed less efficient and exhibited only low enzyme activity and was therefore diluted at 0.65 mg/ml) in albumin buffer was heated at the indicated temperatures for 30 min and immediately cooled down on ice prior to ASL activity measurement. ASL activity indicates in percentage of activity of respective protein heated at 37 °C. The horizontal dashed line marks 50 % of ASL activity, whereas the vertical dashed lines crossing the X-axis indicate the temperatures (V_{50}) at which 50 % of each protein is inactivated. The value V_{50} (°C) was determined by Boltzmann sigmoidal analysis after curve fitting using GraphPad Prism 4. All assays were carried out in triplicate. *Error bars* indicate the standard deviation

Table 1 and Fig. 2c). The normalized maximal reaction velocity (V_{max}) value in cells expressing recombinant mutant protein p.Arg95Cys showed about 13 % of that in cells expressing ASL WT, whereas the other five changes (p.Ile100Thr, p.Val178Met, p.Glu189Glp, Val335Leu and p.Arg379Cys) exhibited ≥58 % of V_{max} of ASL WT. Moreover if compared with WT, the V_{max} values of mutations were consistent with their residual activities and were all significantly lower

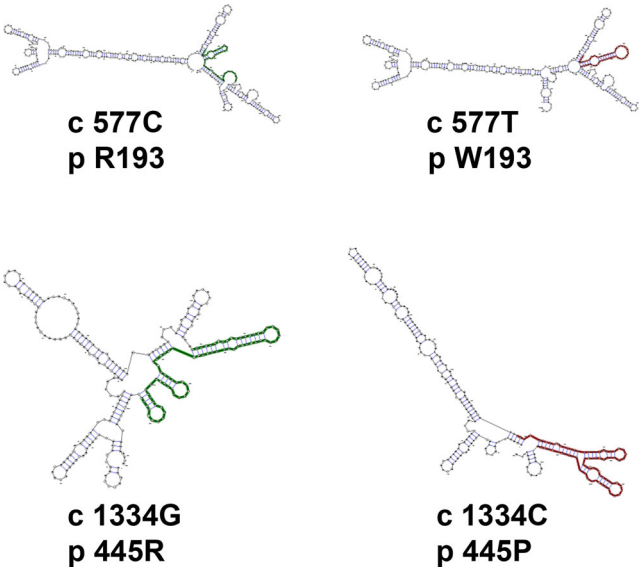

Fig. 3 A comparison of the WT and mutant RNA secondary structures of the R193W and R445P variants. The minimum free energy structure of the WT and mutant RNA were used to provide graphical representation of the secondary structures. The wild-type RNA is shown in green

($p<0.05$). Interestingly, K_m values were not significantly changed in p.Ile100Thr (0.46 mM), p.Val178Met (0.44 mM), p.Glu189Gly (0.49 mM) and p.Val335Leu (0.53 mM). In contrast, K_m values were even slightly decreased in p.Arg95Cys (0.18 mM) and p.Arg379Cys (0.25 mM) compared with that of ASL WT (0.44 mM) indicating an increased substrate affinity in these two mutations. Furthermore, the ratios of V_{max}/K_m in four changes (p.Arg95Cys, p.Ile100Thr, p.Glu189Gly and p.Val335Leu) were decreased (32 %, 61, 78 and 48 % of ASL WT, respectively), while p.Val178Met and p.Arg379Cys showed similar V_{max}/K_m ratios (93 and 112 %, respectively) compared to that of WT indicating an unchanged catalytic efficiency in these mutations.

Variant mutations with high residual ASL activities exhibit thermal instability

In order to further investigate the molecular basis in variant ASL mutations with significant residual activity, we measured the thermal stability of mutant proteins by incubating the protein at different temperatures prior to activity determination (summary of data in Table 1 and Fig. 2d). The T_m values, indicating the temperatures at which 50 % of ASL activity is lost, dropped to 46.5, 48.5, 49.9, 48.1, 42.4 and 48.0 °C for p.Arg95Cys, p.Ile100Thr, p.Val178Met, p.Glu189Gly, p.Val335Leu and p.Arg379Cys, respectively, compared with ASL WT (52.7 °C). All V_{50} values of mutations were significantly decreased ($p<0.05$) suggesting thermal instability of these ASL variants.

Interpretation of the effects of the ASL mutations on the basis of ASL structure

We analysed the effect of mutated residues in human ASL by in-silico mutagenesis of known x-ray crystal structures of ASL protein as template. We also compared human, horse, cow, cat, pig, chimpanzee, dog and rat ASL protein sequences, and amino acids near the substrate binding site and interaction points of the tetrameric protein complex were checked for conservation (Supplementary Fig. 1). Amino acids involved in substrate access and catalysis were conserved across species and no structurally significant substitutions were observed in any of the sequences analysed (Supplementary Fig. 1). A high resolution x-ray crystal structure of ASL that describes the conformations and topologies of ASL monomers has been described by Sampaleanu et al (Sampaleanu et al 2001) which formed the basis of our structural analysis. The enzymatically active form of ASL is a homotetramer which is formed by four identical monomer units which have three distinct helix rich subdomains (Fig. 4) (Sampaleanu et al 2001).

The location of ASL mutations studied in this report on one subunit is depicted in Fig. 4. We performed in-silico mutagenesis on the crystal structure of ASL to generate models of 13 ASL mutations (Supplemental Figs. 2–5) in which amino acids were mutated and side-chains of mutated residues were optimized by MD simulations. Each refined structure was evaluated for a variety of structural parameters like breaking of salt-bridges and hydrogen bonds, changes in charge, size and volume of the altered amino acid and interaction with neighbouring residues, to evaluate the impact of mutations as described previously for several other proteins and structures (Flück et al 2009; Pandey et al 2007; Pandey and Mullis 2011). A detailed description of the predicted properties of the ASL mutations is provided in the Supplementary material and is only summarized in the following.

The arginine 12 residue is located on the highly flexible N-terminus loop in the ASL and showed hydrogen bonding networks with several residues on different ASL subunits. Distortions in the N-terminus loop caused by the mutation of arginine 12 may lead to disruption of ASL substrate binding leading to a loss of activity. This mutation has been reported to cause a milder form of disease but showed only 4.3 % of WT activity in our assays and K_m/V_{max} values could not be accurately determined due to low activity. The aspartate 31 residue is part of the access channel in ASL and had severe loss of activity in our assays. Patients harbouring aspartate to asparagine mutation showed late onset ASL deficiency and mental retardation. The arginine 95 residue has a role in structural stability of ASL and its mutation to cysteine leads to an unstable protein as observed in our experiments. Interestingly the K_m values were lower suggesting a wider substrate access site but loss of stability also led to greatly lower V_{max} values

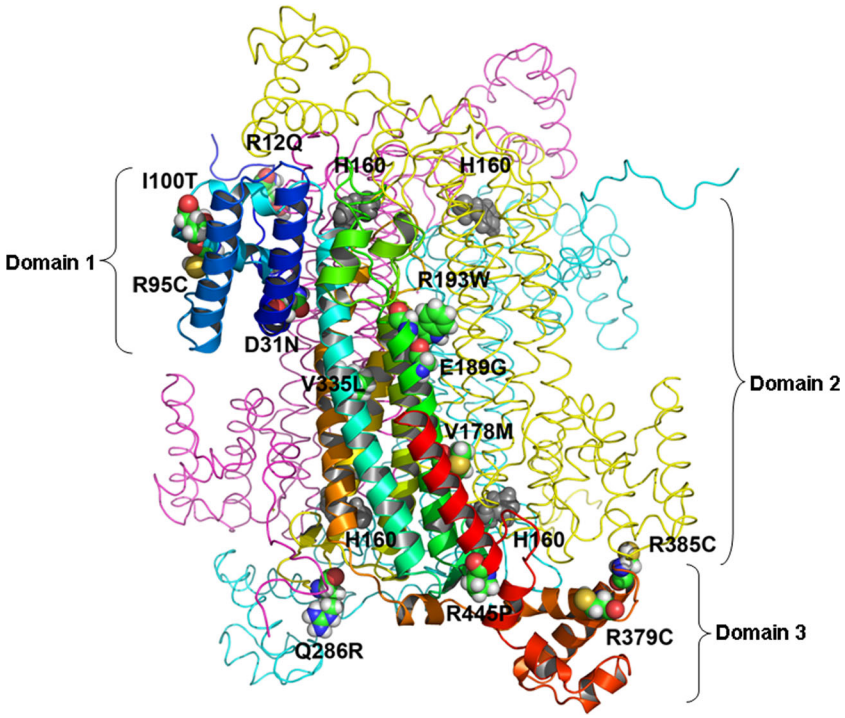

Fig. 4 Three dimensional structure of ASL tetramer showing overall structure of ASL tetramer and the location of mutations on one subunit. Monomeric structure of WT ASL has three distinct subdomains. Domains 1 and 3 have similar structure and topology with two helix-turn-helix motifs in perpendicular arrangement. Domain 2 has nine helices and five of them form the central five helix bundle with up-down-up-down-up topology. In the ASL homotetramer, active site residues are contributed by three different subunits. ASL structure is shown as a ribbons model with different subunits coloured in *rainbow*, *cyan*, *magenta* and *yellow*. The rainbow and cyan subunits form a dimer and join with another dimer formed by magenta and yellow subunits to form the tetramer. Active site residues from one of the sites are shown as solid surfaces while catalytic centre (H160) is shown as spheres. For clarity, helices and sheets are only shown for one subunit shown in rainbow colours *violet* at N-terminus and *red* at C-terminus. The mutations studied in this report are shown as ball and stick models. Each active site is formed by residues from three different monomeric subunits, with contributions from three conserved sequences coming from a different subunit. The histidine 160 residues at the catalytic centres are shown for each subunit

affecting the overall activity of this variant, but sufficient residual activity would be consistent with a milder form of disease. The isoleucine 100 residue was not found to have any direct role in substrate binding or catalysis and its mutation to threonine did not influence K_m but had ~40 loss of activity. The valine 178 residue is part of the central helix bundle forming the core ASL structure but its mutation to methionine did not have any significant effect on ASL activity as per its clinical phenotype of a milder form of ASLD. Several other residues located nearby on the core helix bundle interact via salt-bridge formations and compensate for the structural instability that may arise due to mutation. The glutamate 189 and arginine 193 are involved in structural stability of the central helix bundle of the ASL tetramer. We found that loss of glutamate interaction with arginine 193 of an adjacent ASL subunit was compensated by strong ionic interactions between glutamate 185 and arginine 193 on opposing ASL subunits. Mutation of glutamine to glycine had only a mild effect on V_{max} and K_m values were unchanged which is consistent with a mild clinical phenotype. However, mutation of arginine 193 was found to cause disruption of the core structure of ASL tetramer due to loss of salt bridges with glutamate 185 and 189 on opposing ASL subunits. The arginine 193 to tryptophan mutant had severe loss of activity and K_m/V_{max} values could not be determined accurately due to low activity. The glutamine 286 residue has been studied before and shows severe loss of activity due to disruption of substrate binding site. The valine 335 residue is involved in multiple hydrophobic interactions and contributes to the overall protein stability. The valine 335 mutation to leucine had no impact on substrate binding as expected but had somewhat lower V_{max} values which would indicate structural instability as confirmed by thermal stability assays. The arginine 379 has a role in the structural stability of ASL monomer. The mutation of arginine 379 to cysteine showed lower K_m for the substrate which could be due to a more flexible active site due to structural instability but V_{max} values were lower than the WT enzyme resulting in overall similar enzyme efficiency (V_{max}/K_m). The arginine 385 residue stabilizes the carboxy terminal helix of ASL monomer and its mutations resulted in severe loss of activity. The arginine 385 mutation to cysteine has been reported to cause a milder phenotype but our kinetic and computational analysis could not explain this phenotype. The arginine 445 residue stabilizes the c-terminus helix of the ASL

monomer and its mutation to proline disrupts interactions with aspartate 152 and glutamate 435 causing structural instability. This mutation showed severe loss of activity and kinetic parameters could not be determined.

In the SDM analysis, where an arbitrarily chosen cut-off of 2 kcal mol^{-1} was used for predicting a disease causing effect, a negative score is indicative of a destabilizing effect while a positive score suggests a stabilizing effect. Using this tool, the p.Ile100Thr, p.Glu189Gly and p.Arg445Pro mutations in ASL were predicted to decrease the structural stability and cause disease (Table 2). Structural stability of the tetramer interface is also crucial for the complex formation which was analysed in detail by looking at ionic interactions and hydrogen bond network of residues at the interface of central helices in tetrameric structure (Supplementary Table 3).

Discussion

The broad clinical and biochemical variability of ASLD has been the subject of various investigations over recent years. The presence of residual enzyme activities was confirmed in different expression systems (Barbosa et al 1991; Engel et al 2012; Hu et al 2013; Sampaleanu et al 2001; Trevisson et al 2009; Walker et al 1990, 1997; Yu et al 2001) and was considered as a factor contributing to the spectrum of disease. On the other hand, the finding of cognitive impairment despite higher ASL activity (Ficicioglu et al 2009) and, in other patients, of normal outcome despite undetectable ASL activities (Mercimek-Mahmutoglu et al 2010) led to the assumption of "no correlation between enzyme activity and neuroclinical outcome" (Erez et al 2011a). This overall inconsistent situation may in part be explained by the variety of methods employed including different enzymatic measurements, direct (Ficicioglu et al 2009; Tomlinson and Westall 1964) as well as indirect (Jacoby et al 1972; Kleijer et al 2002) assays, and likewise different ways of expression, yielding recombinant purified ASL protein from prokaryotic overexpression (Engel et al 2012) as well as eukaryotic systems using yeast (Trevisson et al 2009) or human embryonic kidney 293 T cell lysates (Hu et al 2013).

Table 2 Prediction of protein stability using SDM

ASL mutations	Pseudo ΔΔ G (kcal mol^{-1})
p.Arg12Gln	−0.38
p.Asp31Asn	−0.17
p.Arg95Cys	1.84
p.Ile100Thr	−2.02
p.Val178Met	0.98
p.Glu189Gly	−3.18
p.Arg193Trp	1.29
p.Gln286Arg	−0.29
p.Val335Leu	0.20
p.Arg379Cys	−1.88
p.Arg385Cys	−0.21
p.Arg385Leu	−0.08
p.Arg445Pro	−2.28

Prediction of structural changes were done based on statistical potential energy calculation (Worth et al 2007). In the SDM analysis a negative score is indicative of a destabilizing effect and positive score suggests a stabilizing effect. A cut-off of 2 kcal mol^{-1} was used for predicting a destabilizing effect (in bold). L: loop; H: helix; T: turn

None of the mutations led to the prediction of a gross change in secondary structure of the element where the mutated residue belongs

Here, we exploited our recently established eukaryotic expression system that is based on crude cell extracts of transfected 293 T cells (Hu et al 2013) to study in detail all known variant ASL mutations (Balmer et al 2014). The studied 11 variant and two severe missense mutations represent a substantial proportion of the total 92 known ASL missense mutations of which 25 are known to be associated with a severe phenotype (Balmer et al 2014).

Validating our expression system, we found high levels of ASL enzyme activity in the recombinant WT and levels< 1.5 % of WT in the severe mutations and sufficient expression of all recombinant proteins (Fig. 2a). Interestingly, while most mutations, including the severe changes p.Gln286Arg and p.Arg385Leu, expressed at levels comparable to ASL WT, we found three variant mutations that yielded clearly lower protein expression (p.Arg95Cys, p.Arg193Trp, p.Arg445Pro) indicating their disease causing role and already pointing towards instability of the mutant proteins. The RNA secondary structure may also play a role in lower levels of expression. Therefore, a combination of lower translation as well as protein instability may affect the overall outcome of some ASL variants.

Six (p.Arg95Cys, p.Ile100Thr, p.Val178Met, p.Glu189Gly, p.Val335Leu and p.Arg379Cys) of the 11 variant ASL constructs yielded levels of residual activity ≥18 % of WT (Table 1 and Fig. 2b). Two of these mutations, p.Val178Met and p.Val335Leu, displayed relevant enzyme activities already in yeast expression (Trevisson et al 2009) as well as in the case of p.Val178Met in [^{14}C]citrulline incorporation studies (Kleijer et al 2002). Four of the mutant ASL proteins (p.Ile100Thr, p.Val178Met, p.Glu189Gly and p.Val335Leu) showed no significant changed K_m values and two mutations (p.Arg95Cys and p.Arg379Cys) even displayed slightly decreased K_m values (Table 1), which would explain their milder phenotype. This is in contrast to significantly lowered K_m values obtained in bacterial expression of p.Val178Met and p.Arg379Cys (Engel et al 2012). Four of the mutant ASL proteins (p.R95C, p.Ile100Thr, p.Glu189Gly and p.Val335Leu) showed decreased enzyme efficiency (V_{max}/K_m: 32, 61, 78 and 48 % of ASL WT,

respectively) possibly contributing to the clinical phenotype despite surprisingly high residual activities. For the majority of the mutants studied here, the clinical phenotype, which is at least known for each one or few patients (as summarized in (Balmer et al 2014)), is in accordance with the relevant levels of ASL activity. Exceptions to this comprise the following mutants: mutation p.Arg12Gln would be expected to be associated with rather high levels of ASL activity based on a single report of an asymptomatic individual with the p.Arg12Gln/p.Glu36Glyfs*32 genotype (Balmer et al 2014) but was found with only 4 % of ASL-WT activity. For p.Asp31Asn, there is only information from two patients with late onset ASLD resulting in mental retardation (Trevisson et al 2007) but the data from our expression system for this mutant would rather predict a more severe course. In mutations pArg385Cys and p.Arg445Pro, we consider the residual ASL activity levels as consistent with the available clinical information, which indicate rather severe disease (albeit not always classical neonatal onset) in patients homozygous for p.Arg385Cys while there is only information from one patient available with p.Arg445Pro (Dursun et al 2008). These discrepancies indicate that, although in general a reliable tool, our assay fails to represent in some cases the actual activity in the patient.

In a previous study applying ASL expression in yeast, mutations p.Val178Met and p.Val335Leu were shown by immunoblot analysis to encode for stable proteins (Trevisson et al 2009) and this is confirmed here for most of the variant mutations (Fig. 2a). However in silico modelling of p.Arg95Cys, p.Ile100Thr, p.Glu189Gly, p.Val335Leu and p.Arg379Cys, Q286R and R445P suggested either ASL protein or tetramer instability. The findings of a low expression level for p.Arg95Cys, p.Arg193Trp and p.Arg445Pro, as well as decreased thermal stability for p.Arg95Cys, p.Ile100Thr, p.Glu189Gly, p.Val335Leu and p.Arg379Cys further point towards an unstable ASL protein in the aforementioned mutations. This opens the possibility of stabilizing these mutant proteins by pharmacological chaperones as a new therapeutic approach in ASLD. In studies investigating this, the impact of intragenic complementation (Walker et al 1997; Yu et al 2001) on the efficacy of pharmacological chaperones is difficult to foresee but should not prevent such further work. Since all of the mutations that possibly qualify for chaperone treatment are recurrent and some even belong to the most frequently found mutations in ASLD patients (Balmer et al 2014), identification of compounds that can be used for this purpose should become a research priority. This is underlined by the fact that about 30 % (n=49) of the 160 known different genotypes are affected at least on one allele by any of the mutations described here as possible targets of chaperone treatment.

Our findings are further substantiated by predictions from structure modelling (Supplementary material). The variants studied in this report can be divided in two different groups based on their impact on the structure of the ASL protein. Most of the variants affect the atomic interactions within a monomeric ASL unit while variants p.Glu189Gly and p.Arg193Trp were found to impact the tetramer formation. The enzyme kinetic data and thermal stability analysis were in general agreement with the structural analysis. Mutations with complete or near-complete effects on activity were either near the active site (p.Arg12Gln, p.Asp31Asn, p.Gln286Arg, p.Arg385Cys and p.Arg385Leu) or hampered the structural stability of monomer (p.Arg445Pro) or tetramer (p.Arg193Trp). Two variants near the tetrameric interface, p.Val178Met and p.Glu189Gly did not have severe effects on enzymatic activity. Further computational analysis showed that multiple strong ionic interactions between arginine 193, lysine 192 of one subunit with the glutamate 185 and glutamate 189 of another interacting ASL monomeric unit could compensate for loss of some interactions. The major result of this analysis is the role of arginine 193 in the structural stability of the ASL complex. Involvement of arginine 193 with several adjacent acidic residues meant that any mutation of arginine 193 residue would have a strong negative impact on protein stability and catalytic activity.

In conclusion, we have found significant residual levels of ASL activity in some of the mutations that are associated with a variant clinical and biochemical phenotype of ASLD. Likewise, this study provides evidence for instability of the mutant proteins and adds ASLD to the list of target diseases for novel therapeutic approaches with small molecules allowing scaffolding to improve stability. Based on recent data on the genotypes found in ASLD it is obvious that the search for compounds that stabilize the ASL protein should be pursued with highest priority to eventually gain benefit for a substantial proportion (about 30 %) of ASLD patients.

Acknowledgments The authors are grateful for the technical assistance provided by the late M. Groux, Bern.

Funding This work was supported by the Swiss National Science Foundation [grants No. 310030_127184/1 and 310030_153196/1 to JH and 310031_134926 to AVP] and a grant from Schweizerische Mobiliar Genossenschaft Jubiläumsstiftung to AVP.

Compliance with Ethics Guidelines

Conflict of interest None.

Human and Animal Rights and Informed Consent This article does not contain any studies with human or animal subjects performed by the any of the authors.

References

Balmer C, Pandey AV, Rüfenacht V, Nuoffer JM, Fang P, Wong LJ, Häberle J (2014) Mutations and polymorphisms in the human argininosuccinate lyase (ASL) gene. Hum Mutat 35:27–35

Barbosa P, Cialkowski M, O'Brien WE (1991) Analysis of naturally occurring and site-directed mutations in the argininosuccinate lyase gene. J Biol Chem 266:5286–90

Bowie JU, Luthy R, Eisenberg D (1991) A method to identify protein sequences that fold into a known three-dimensional structure. Science 253:164–70

Bradford MM (1976) A rapid and sensitive method for the quantitation of microgram quantities of protein utilizing the principle of protein-dye binding. Anal Biochem 72:248–54

Brunetti-Pierri N, Erez A, Shchelochkov O, Craigen W, Lee B (2009) Systemic hypertension in two patients with ASL deficiency: a result of nitric oxide deficiency? Mol Genet Metab 98:195–7

Brusilow S, Horwich A (2001) Urea cycle enzymes. In: Scriver C, Beaudet A, Sly W, Valle D (eds) The metabolic & molecular bases of inherited disease, 8th edn. McGraw-Hill, New York, pp 1909–1963

Brusilow SW, Maestri NE (1996) Urea cycle disorders: diagnosis, pathophysiology, and therapy. Adv Pediatr 43:127–70

Doimo M, Trevisson E, Sartori G, Burlina A, Salviati L (2012) Yeast complementation is sufficiently sensitive to detect the residual activity of ASL alleles associated with mild forms of argininosuccinic aciduria. J Inherit Metab Dis 35:557–8

Dursun A, Sivri HS, Ozon A, Akcaören Z, Tokatly A, Koch HG, Coskun T (2008) Argininosuccinic aciduris associated with pancreatitis (abstract). J Inherit Metab Dis 31(Supp. 1):90

Engel K, Vuissoz JM, Eggimann S, Groux M, Berning C, Hu L, Klaus V, Moeslinger D, Mercimek-Mahmutoglu S, Stockler S, Wermuth B, Häberle J, Nuoffer JM (2012) Bacterial expression of mutant argininosuccinate lyase reveals imperfect correlation of in-vitro enzyme activity with clinical phenotype in argininosuccinic aciduria. J Inherit Metab Dis 35:133–40

Erez A, Nagamani SC, Lee B (2011a) Argininosuccinate lyase deficiency-argininosuccinic aciduria and beyond. Am J Med Genet C: Semin Med Genet 157:45–53

Erez A, Nagamani SC, Shchelochkov OA, Premkumar MH, Campeau PM, Chen Y, Garg HK, Li L, Mian A, Bertin TK, Black JO, Zeng H, Tang Y, Reddy AK, Summar M, O'Brien WE, Harrison DG, Mitch WE, Marini JC, Aschner JL, Bryan NS, Lee B (2011b) Requirement of argininosuccinate lyase for systemic nitric oxide production. Nat Med 17:1619–26

Ficicioglu C, Mandell R, Shih VE (2009) Argininosuccinate lyase deficiency: longterm outcome of 13 patients detected by newborn screening. Mol Genet Metab 98:273–7

Flück CE, Mullis PE, Pandey AV (2009) Modeling of human P450 oxidoreductase structure by in silico mutagenesis and Md simulation. Mol Cell Endocrinol 313:17–22

Hooft RW, Vriend G, Sander C, Abola EE (1996) Errors in protein structures. Nature 381:272

Hooft RW, Sander C, Vriend G (1997) Objectively judging the quality of a protein structure from a Ramachandran plot. Comput Appl Biosci 13:425–30

Hu L, Pandey AV, Eggimann S, Rüfenacht V, Moslinger D, Nuoffer JM, Häberle J (2013) Understanding the role of argininosuccinate lyase transcript variants in the clinical and biochemical variability of the urea cycle disorder argininosuccinic aciduria. J Biol Chem 288: 34599–611

Jacoby LB, Littlefield JW, Milunsky A, Shih VE, Wilroy RS Jr (1972) A microassay for argininosuccinase in cultured cells. Am J Hum Genet 24:321–4

Kleijer WJ, Garritsen VH, Linnebank M, Mooyer P, Huijmans JG, Mustonen A, Simola KO, Arslan-Kirchner M, Battini R, Briones P, Cardo E, Mandel H, Tschiedel E, Wanders RJ, Koch HG (2002) Clinical, enzymatic, and molecular genetic characterization of a biochemical variant type of argininosuccinic aciduria: prenatal and postnatal diagnosis in five unrelated families. J Inherit Metab Dis 25:399–410

Krieger E, Darden T, Nabuurs SB, Finkelstein A, Vriend G (2004) Making optimal use of empirical energy functions: force-field parameterization in crystal space. Proteins 57:678–83

Laemmli UK (1970) Cleavage of structural proteins during the assembly of the head of bacteriophage T4. Nature 227:680–5

Linnebank M, Tschiedel E, Häberle J, Linnebank A, Willenbring H, Kleijer WJ, Koch HG (2002) Argininosuccinate lyase (ASL) deficiency: mutation analysis in 27 patients and a completed structure of the human ASL gene. Hum Genet 111:350–9

Liu H, Elstner M, Kaxiras E, Frauenheim T, Hermans J, Yang W (2001) Quantum mechanics simulation of protein dynamics on long timescale. Proteins 44:484–9

Luthy R, Bowie JU, Eisenberg D (1992) Assessment of protein models with three-dimensional profiles. Nature 356:83–5

Mercimek-Mahmutoglu S, Moeslinger D, Häberle J, Engel K, Herle M, Strobl MW, Scheibenreiter S, Muehl A, Stockler-Ipsiroglu S (2010) Long-term outcome of patients with argininosuccinate lyase deficiency diagnosed by newborn screening in Austria. Mol Genet Metab 100:24–8

Mori T, Nagai K, Mori M, Nagao M, Imamura M, Iijima M, Kobayashi K (2002) Progressive liver fibrosis in late-onset argininosuccinate lyase deficiency. Pediatr Dev Pathol 5:597–601

O'Brien WE, Barr RH (1981) Argininosuccinate lyase: purification and characterization from human liver. Biochemistry 20:2056–60

O'Brien WE, McInnes R, Kalumuck K, Adcock M (1986) Cloning and sequence analysis of cDNA for human argininosuccinate lyase. Proc Natl Acad Sci U S A 83:7211–5

Palekar AG, Mantagos S (1981) Human liver arginiosuccinase purification and partial characterization. J Biol Chem 256:9192–4

Pandey AV, Mullis PE (2011) Molecular genetics and bioinformatics methods for diagnosis of endocrine disorders. In: Ranke MB, Mullis PE (eds) Diagnostics of endocrine function in children and adolescents, 4th edn. Karger, Basel, pp 1–21

Pandey AV, Kempna P, Hofer G, Mullis PE, Flück CE (2007) Modulation of human CYP19A1 activity by mutant NADPH P450 oxidoreductase. Mol Endocrinol 21:2579–95

Ramachandran GN, Ramakrishnan C, Sasisekharan V (1963) Stereochemistry of polypeptide chain configurations. J Mol Biol 7: 95–9

Sabarinathan R, Tafer H, Seemann SE, Hofacker IL, Stadler PF, Gorodkin J (2013) RNAsnp: efficient detection of local RNA secondary structure changes induced by SNPs. Hum Mutat 34:546–56

Sampaleanu LM, Vallee F, Thompson GD, Howell PL (2001) Three-dimensional structure of the argininosuccinate lyase frequently complementing allele Q286R. Biochemistry 40: 15570–80

Shulman-Peleg A, Nussinov R, Wolfson HJ (2004) Recognition of functional sites in protein structures. J Mol Biol 339:607–33

Shulman-Peleg A, Nussinov R, Wolfson HJ (2005) SiteEngines: recognition and comparison of binding sites and protein-protein interfaces. Nucleic Acids Res 33:W337–41

Smith RE, Lovell SC, Burke DF, Montalvao RW, Blundell TL (2007) Andante: reducing side-chain rotamer search space during comparative modeling using environment-specific substitution probabilities. Bioinformatics 23:1099–105

Solitare GB, Shih VE, Nelligan DJ, Dolan TF Jr (1969) Argininosuccinic aciduria: clinical, biochemical, anatomical and neuropathological observations. J Ment Defic Res 13:153–70

Tanaka T, Nagao M, Mori T, Tsutsumi H (2002) A novel stop codon mutation (X465Y) in the argininosuccinate lyase gene in a patient with argininosuccinic aciduria. Tohoku J Exp Med 198:119–24

Todd S, McGill JR, McCombs JL, Moore CM, Weider I, Naylor SL (1989) cDNA sequence, interspecies comparison, and gene mapping analysis of argininosuccinate lyase. Genomics 4:53–9

Tomlinson S, Westall RG (1960) Argininosuccinase activity in brain tissue. Nature 188:235–6

Tomlinson S, Westall RG (1964) Argininosuccinic aciduria. Argininosuccinase and arginase in human blood cells. Clin Sci 26: 261–9

Topham CM, Srinivasan N, Blundell TL (1997) Prediction of the stability of protein mutants based on structural environment-dependent amino acid substitution and propensity tables. Protein Eng 10:7–21

Trevisson E, Salviati L, Baldoin MC, Toldo I, Casarin A, Sacconi S, Cesaro L, Basso G, Burlina AB (2007) Argininosuccinate lyase deficiency: mutational spectrum in Italian patients and identification of a novel ASL pseudogene. Hum Mutat 28:694–702

Trevisson E, Burlina A, Doimo M, Pertegato V, Casarin A, Cesaro L, Navas P, Basso G, Sartori G, Salviati L (2009) Functional complementation in yeast allows molecular characterization of missense argininosuccinate lyase mutations. J Biol Chem 284:28926–34

Vallee F, Turner MA, Lindley PL, Howell PL (1999) Crystal structure of an inactive duck delta II crystallin mutant with bound argininosuccinate. Biochemistry 38:2425–34

Vriend G (1990) WHAT IF: a molecular modeling and drug design program. J Mol Graph 8(52–6):29

Walker DC, McCloskey DA, Simard LR, McInnes RR (1990) Molecular analysis of human argininosuccinate lyase: mutant characterization and alternative splicing of the coding region. Proc Natl Acad Sci U S A 87:9625–9

Walker DC, Christodoulou J, Craig HJ, Simard LR, Ploder L, Howell PL, McInnes RR (1997) Intragenic complementation at the human argininosuccinate lyase locus. Identification of the major complementing alleles. J Biol Chem 272:6777–83

Worth CL, Bickerton GR, Schreyer A, Forman JR, Cheng TM, Lee S, Gong S, Burke DF, Blundell TL (2007) A structural bioinformatics approach to the analysis of nonsynonymous single nucleotide polymorphisms (nsSNPs) and their relation to disease. J Bioinforma Comput Biol 5:1297–318

Yu B, Thompson GD, Yip P, Howell PL, Davidson AR (2001) Mechanisms for intragenic complementation at the human argininosuccinate lyase locus. Biochemistry 40:15581–90

Zimmermann A, Bachmann C, Baumgartner R (1986) Severe liver fibrosis in argininosuccinic aciduria. Arch Pathol Lab Med 110:136–40